Next-generation hollow retroreflectors for lunar laser ranging

Alix Preston and Stephen Merkowitz*

Goddard Space Flight Center, 8800 Greenbelt Rd., Greenbelt, Maryland 20771, USA

*Corresponding author: stephen.m.merkowitz@nasa.gov

Received 20 September 2013; revised 17 November 2013; accepted 19 November 2013; posted 20 November 2013 (Doc. ID 198004); published 13 December 2013

The three retroreflector arrays put on the Moon 40 years ago by the Apollo astronauts and the French-built arrays on the Soviet Lunokhod rovers continue to be useful targets, and have provided the most stringent tests of the Strong Equivalence Principle and the time variation of Newton's gravitational constant, as well as valuable insight into the Moon's interior. However, the precision of the ranging measurements are now being limited by the physical size of the arrays and a new generation of retroreflectors is required to make significant advances over current capabilities. Large single-cube retroreflectors represent the most promising approach to overcoming current limitations, and hollow retroreflectors in particular have the potential to maintain their good optical performance over the nearly 300 K temperature swing that occurs during the lunar cycle. Typically, epoxies are used for aligning and bonding hollow retroreflectors, but their thermal stability will predominantly be limited by the difference of the coefficient of thermal expansion (CTE) between the epoxy and the glass. A relatively new bonding method known as hydroxide catalysis bonding (HCB) has been used to adhere complex optical components for space-based missions. HCB has an extremely thin bond, a low CTE, and a high breaking strength that makes it an ideal candidate for bonding hollow retroreflectors for lunar laser ranging (LLR). In this work, we present results of a feasibility study of bonded Pyrex and fused silica hollow retroreflectors using both epoxy and HCB methods, including the results of thermally cycling the hollow retroreflectors from 295 to 185 K. Finally, we discuss the potential for using these retroreflectors for future LLR. © 2013 Optical Society of America

OCIS codes: (080.4035) Mirror system design; (120.6085) Space instrumentation; (120.3930) Metrological instrumentation; (220.1140) Alignment.

http://dx.doi.org/10.1364/AO.52.008676

1. Introduction

Over the past four decades, laser ranging to the retroreflector arrays placed on the lunar surface by the Apollo astronauts and the Soviet Luna missions have dramatically increased our understanding of gravitational physics along with Earth and Moon geophysics, geodesy, and dynamics [1,2]. During that time, the precision of the range measurements has improved each time the ground stations were upgraded to the most advanced ranging technology at the time. This is despite the fact that the efficiency of the arrays appears to have degraded by a factor of 10 [3]. Incredibly, it has taken nearly 40 years for the ground stations to catch up with the potential capability of the original retroreflector arrays.

Improvements in the geometric coverage, both on Earth and on the Moon, will have a direct impact on the science gained through lunar laser ranging (LLR). Studies of the structure and composition of the interior require measurements of the lunar librations, while tests of general relativity require the position of the lunar center of mass. In all, 6 degrees of freedom are required to constrain the geometry of the Earth–Moon system (in addition to Earth orientation). A single ranging station and reflector are insufficient to accurately determine all 6 degrees of

1559-128X/13/368676-09$15.00/0
© 2013 Optical Society of America

freedom, even given the rotation of the Earth with respect to the Moon. The addition of one or more reflectors and one or more additional ranging stations in the Earth's southern hemisphere would strengthen the geometric coverage and increase the sensitivity to lunar motion by as much as a factor of 4 in some degrees of freedom at the same level of ranging precision [4]. The rediscovery of Lunokhod 1 will also greatly improve the geometric coverage, and consequently, the science return [5].

Since 1969, several stations have successfully ranged to the lunar retroreflectors and have increased the range precision from about 20 cm to just a few centimeters [2,6,7]. Poor detection rates have historically limited LLR precision (not every laser pulse sent to the Moon results in a detected return photon). However, the relatively new APOLLO system has been able to increase detection rates, leading to a statistical uncertainty of about 1 mm for timescales of less than 10 min [8].

The dominant random uncertainty per photon received by APOLLO stems from the physical size of the arrays and their changing orientation due to the lunar librations. The incoming pulse from APOLLO will illuminate an entire array, but only one (sometimes a few) of the photons will be detected upon return. APOLLO cannot determine what area of the array contributed most of the returned light, so the tilt of the array with respect to the Earth spreads out the distribution of laser pulses. The typical array dimension (Apollo 11 and 14) of 0.5 m and a typical libration angle of 6 deg translates to a full-width pulse-spread of about 330 ps in the roundtrip time. As the Moon librates, the amount of spreading changes since the array is also changing its orientation with respect to the ground station.

Modest improvements in the ranging technology will not significantly improve the range precision, as the array tilt will continue to dominate the error budget for the foreseeable future. In addition, new arrays with more (or less) cubes of the same size would result in no gain: doubling the physical dimension doubles the random uncertainty, requiring four times as many photons, exactly what doubling the linear array dimension provides. Likewise, the reduction in return photons would eliminate any benefit of choosing a smaller array. The solution is to deploy large single cubes (7–10 cm) that have similar lidar cross-sections to the Apollo arrays, but will not produce significant pulse spreading.

However, the temperature dependence of the cube material's index of refraction makes the scaling up of traditional solid retroreflectors particularly challenging [9,10]. A promising alternative is to use hollow (open) cube corners. Since hollow cubes are reflective, the index of refraction problem goes away. They also do not introduce significant polarization effects. Therefore, they can be made larger without significantly sacrificing optical performance.

Hollow cubes have flown on a few space missions, but are generally not used on satellites for laser ranging because of a lack of test data and some indications of instabilities at high temperatures. These instabilities are likely a result of the use of epoxy to bond the mirrors; the large differences in the coefficient of thermal expansion (CTE) and stresses within the epoxy may cause the retroreflector to distort with temperature changes and temperature gradients. A potential solution is to replace the epoxy with a bond material that has a similar CTE to that of the glass mirrors, such as hydroxide catalysis bonding (HCB). HCB was developed for the Gravity Probe B mission to bond the fused silica pieces that form the star-tracking telescope [11–13]. Since then, HCB has been shown to be successful for many other materials and applications [14–16]. The thin bond, high strength, and low CTE make it ideal for bonding hollow retroreflectors for use with LLR [17,18]. In this work, we present the results of a feasibility study on the fabrication of hollow retroreflectors for use with LLR made using both epoxy bonding and HCB methods. In addition, we present results from thermally cycling these hollow retroreflectors from 295 to 185 K and show that these results are as good as or better than those of the hollow retroreflectors for the CIRS instrument on the Cassini spacecraft [19], which, to the authors' knowledge, are the best results that have been published so far.

2. Corner Cube Fabrication

A total of 12 hollow retroreflectors were made. Ten were made of a borosilicate material equivalent to that of Pyrex, and two were made out of fused silica. Of the 10 Pyrex retroreflectors, 4 were bonded using an epoxy, 3 using HCB, and 3 using a hybrid method where a small amount of epoxy was applied first and then a hydroxide solution was applied afterward. Both fused silica retroreflectors were bonded using HCB. The physical properties of these cubes are presented in Table 1 and a brief description of the bonding process for each type of cube is given in the following subsections.

A. Epoxy-Bonded Retroreflectors

A Verifire XPZ interferometer (ZYGO Corp.) was used to measure the dihedral angle errors of the three right angles in real time when bonding the retroreflectors. An aluminum fixture that allowed the three dihedral angles to be independently adjusted was used to align the retroreflectors. Mirror panels 38.1 mm × 39.4 mm × 6.4 mm made of a borosilicate equivalent to Pyrex were bonded to the fixture to provide a rigid structure while the mirrors were being aligned. Each mirror had a reflective face that was coated with a protected aluminum coating and had a peak-to-valley (PV) surface roughness ranging from $\lambda/4$ to $\lambda/8$ (at 633 nm). The mirrored face had three beveled edges and one knife edge that was used to sit on the next panel's mirrored surface where the bonding took place. This produced a bonding seam approximately 1.3 mm thick, for the length of the mirror, that consisted of a ground surface being

Table 1. Properties of the Hollow Retroreflectors Before Thermal Cycling

Retro	Material	Bonding Method	Dihedral Angle Error (arc sec)	Wavefront (PV at 633 nm)	Max. Beam Deviation (arc sec)
E1	Pyrex equiv.	Epoxy	−0.1,0.0,−1.4	1.28	5.8
E2	Pyrex equiv.	Epoxy	−0.9,0.0,−1.8	1.49	6.6
E3	Pyrex equiv.	Epoxy	0.4,3.7,2.8	2.97	12.9
E4	Pyrex equiv.	Epoxy	3.6,0.3,3.7	2.60	13.0
HCB1	Pyrex equiv.	HCB	−15.6,1.7,4.5	5.16	32.3
HCB2	Pyrex equiv.	HCB	8.7,13.8,−3.2	5.72	34.8
HCB3	Pyrex equiv.	HCB	0.8,12.5,20.4	9.69	55.9
H1	Pyrex equiv.	Hybrid	24.7,32.5,35.2	20.84	122.1
H2	Pyrex equiv.	Hybrid	3.5,9.8,3.5	4.89	24.7
H3	Pyrex equiv.	Hybrid	10.0,13.2,6.9	6.52	39.5
FS1	Fused silica	HCB	−1.9,0.3,−8.4	2.92	19.5
FS2	Fused silica	HCB	1.9,1.7,3.1	1.46	10.5

bonded to a mirrored surface. In this way, none of the dihedral angles were constrained by the geometry of the retroreflector itself. Since the dihedral angles were unconstrained by the retroreflector geometry, the fixture could be used to control each of the three dihedral angles independently during the assembly and bonding process. The epoxy used was Epon/Versamid in a 50/50 mixture that had been mixed at Appli-tec and cryogenically stored before use. A paint brush was used to apply a small amount of epoxy to the bonding seam. Active alignment of the cube took place for anywhere between 4 and 6 h after the epoxy had been applied, and then was left to cure overnight before being taken out of the fixture.

In the case of retroreflector E4, a small groove approximately 1.9 mm wide and 1.3 mm deep was cut down the middle of the surface that had the knife edge. The same bonding procedure as described before was used, but instead of using a 1.3 mm bonding overlap, the entire thickness of the mirror panel was overlapped onto the adjacent mirror surface. Epoxy was placed on the edges of the groove and the alignment was done in the same manner as described previously.

B. HCB Retroreflectors

The epoxy bonding technique described was found to be ineffective for HCB using a thin bonding overlap. The dihedral angles would either increase beyond the measurement range of the interferometer (i.e., "flower open"), or the retroreflector would fall apart after taking the retroreflector out of the fixture. This was attributed to the small width, and hence total area, of the bonding seam. Significantly better results were achieved after increasing the bond width to greater than 4 mm. Once the bond width was increased, the retroreflectors did not flower open as much, but obtaining perpendicular dihedral angles was still extremely difficult (see Table 1). To bond the retroreflectors using HCB, the mirrors were put into the fixture in the same manner as when epoxy bonding was used, but instead of a 1.3 mm bonding seam, the mirrors were set such that the bonding seam was 4 mm wide. Once this was done, a brush was dipped into a sodium silicate solution. This solution was made by volumetrically diluting stock sodium silicate solution (Sigma-Aldrich, part number 338443) by a factor of 1:4. The brush was then touched to the bonding seam and the solution was allowed to wick in. The retroreflector was then actively aligned underneath the interferometer for approximately 1 h and left to sit in the fixture for at least 8 days before it was taken out of the fixture. Using this method, we were able to produce retroreflectors with the physical properties shown in Table 1 for retroreflectors HCB1, HCB2, and HCB3.

It was speculated by the authors that the rough bonding surface was causing the dihedral angle errors to be much greater than those when epoxy bonding was used. To test this, mirror panels that had a perpendicular, smooth, and flat bonding surface were used to bond two retroreflectors. These mirrors were made by cutting a 6.35 mm thick slice from a solid fused silica retroreflector that had dihedral angle errors less than 3 arc sec (Edmund Optics, part number 49-011). Each slice was then coated with a protected aluminum coating. These mirrors were then situated in the fixture such that the full 6.35 mm width was on the mirrored surface approximately 1 mm from the end of the mirror (see Fig. 1). Once the mirrors were aligned in the fixture, 0.15 μL of 1:4 sodium silicate solution was applied to the bonding seam. The solution was allowed to wick in and

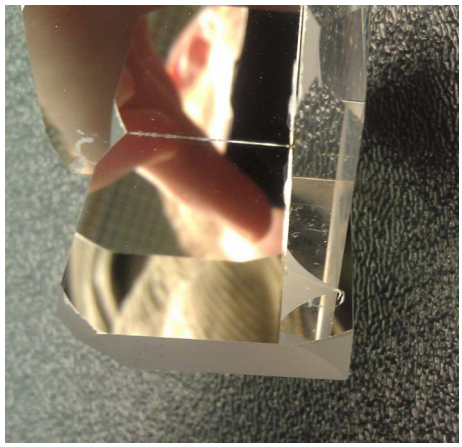

Fig. 1. Bonded fused silica retroreflector showing the placement of the mirrors, bond width, and spacing before the edge.

the excess was soaked up with a Q-tip. The retroreflector was not actively aligned and sat in the fixture for two weeks while the bonds cured. After two weeks, the retroreflector was taken out of the fixture. Its physical properties are given in Table 1 for retroreflector FS1.

In addition to bonding the fused silica panels using the fixture, another cube was made from the fused silica panels using a solid "master cube" as a mandrel. The master cube was a solid retroreflector made from BK7 and had dihedral angles polished to better than 1 arc sec. The edges were beveled to make sure that any solution that may leak out would not get onto the master cube and bond to it. The fused silica mirrors were stripped of their protected aluminum coating and placed on the master cube in the same configuration as described for the other fused silica retroreflector. Plastic screws that had been rounded at the tips were used to hold the fused silica panels in place while the other panels were being adjusted. Interference fringes between the master cube and the fused silica panels, as well as where the bonding would take place, were used to determine how well aligned the panels were. A bonding solution was made by diluting a stock potassium hydroxide solution (Fisher Scientific, part number SP236-500) with deionized water such that the molecular ratio of potassium hydroxide to water was 1:128. This solution was applied to the bond areas using a brush, and the retroreflector cured at room temperature for 20 days and then was taken off of the master cube. A protected aluminum coating was then applied to the surfaces. The resulting properties for this cube are shown in Table 1 for retroreflector FS2.

C. Hybrid Retroreflectors

A technique that combined epoxy and HCB was also developed. This was motivated by the fact that the dihedral angles would change in a very unpredictable manner when HCB was used to bond rough surfaces. The dihedral angle could be set more accurately using a small amount of epoxy on the sides of the retroreflectors and still allow for a small amount of adjustment (typically a few arc seconds). The hydroxide solution was added after the epoxy was left to cure for a few days, and only a small amount of active alignment was usually required. In this manner, the hydroxide bond should be stronger since there is more of it and it is spread out over a larger area, so it should counteract the effects of the epoxy when thermally cycled. For retroreflector H1, only half of the thickness of the mirror was epoxied (as shown on the left side of Fig. 2) while, for retroreflector H2, the entire thickness of the mirror was epoxied. Finally, for retroreflector H3, a groove similar to retroreflector E4 was machined down the middle and the ends were epoxied (right side of Fig. 2). After the epoxy bond had cured, 0.15 μL of 1:4 sodium silicate solution was applied in the groove and allowed to wick into the surrounding bonding area. The physical properties of these cubes are given in Table 1.

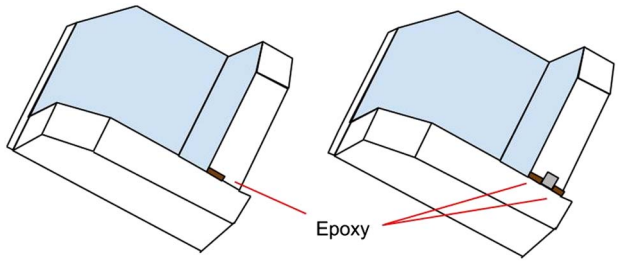

Fig. 2. Placement of the epoxy for retroreflectors H1 (left) and H3 (right).

3. Experimental Setup

To determine how well the different bonding techniques and materials performed when thermally cycled, all of the retroreflectors were thermally cycled from 295 to 185 K. The thermal vacuum chamber used to thermally cycle the retroreflectors is shown in Fig. 3. Chilled air from a liquid nitrogen dewar was funneled so that it blew against a brass cooling plate. On the other side of the cooling plate was an aluminum mount that was enclosed by a vacuum chamber. The retroreflector sat in an aluminum mount such that the aluminum panels were approximately 1–2 mm from the back of the retroreflector. The retroreflector sat on thin strips of Ultem to restrict the conductive heat flow, and the entire structure was surrounded with layers of thermal shielding. In this manner, the method of cooling was predominantly through radiative heat transfer while not distorting the retroreflector as it is cooled. The temperature of the brass cooling plate and the retroreflectors were both measured using temperature sensors and thermocouple reader (Lake Shore temperature controller 330) during the entire thermal cycle. The retroreflectors were cooled from 295 to 185 K at approximately 1–2 K/min and then the air flow from the liquid nitrogen dewar was cut off and the retroreflector was allowed to warm back up to 295 K. As the retroreflector was being cooled, the temperature differential between the brass cooling plate and the retroreflector was approximately 30–40 K. As the retroreflector warmed up and reached a temperature of 195 K, the brass plate was typically within 6 K of the retroreflector. A Verifire XPZ interferometer was used to measure the

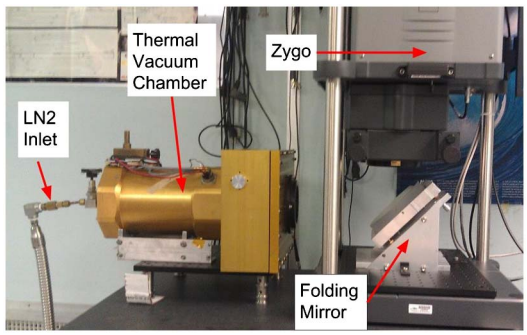

Fig. 3. Thermal vacuum chamber used to thermally cycle the hollow retroreflectors.

dihedral angle errors, wavefront, and maximum beam deviation (MBD) of the retroreflector before the cooling began, after it had been cooled to its minimum, then back through 195 K, and finally after returning to 295 K. To make the data easier to understand, in the following tables the initial values of the dihedral angles, wavefront, and MBD are all set to zero and are not shown. The change from the initial values after being cooled and then passing through 195 K are given in the third, fifth, and seventh columns of the following tables, and the change from the initial values after warming back up to 295 K are given in the fourth, sixth, and eighth columns. The data after returning to 295 K from being cooled is needed, since many of the retroreflectors did not return to their original positions after being thermally cycled, and is discussed in the next section.

Due to the vibrational noise of the system, only single-phase measurements could be taken while in single-pass mode. These measurements were taken from 194.5 to 195.5 K and typically included 5–6 phase measurements. The averages of these measurements were calculated and used in Tables 2–5. The typical errors associated with these measurements were ±0.15 to ±0.35 arc sec for the dihedral angle errors, ±0.05 to ±0.15 waves for the wavefront measurements, and ±0.20 to ±0.35 arc sec for the MBD.

4. Results and Discussion

A. Epoxy-bonded Retroreflectors

The results of thermally cycling the epoxied retroreflectors are presented in Table 2. The data presented in the third and fourth columns of Table 2 are the total dihedral angle change. This corresponds to the amount of change for each dihedral angle being added for all three dihedral angles. For example, if the dihedral angle errors before testing are (−1.0, 0.0, 0.5) and then, after being cooled to 195 K, they are (−2.0, 0.5, 0.0), then the total dihedral angle change is $|-2.0-(-1.0)|+|0.5-0.0|+|0.0-0.5|=2$ arc sec.

As seen in the data presented in Tables 2–5, most samples were exposed to either three or four full thermal cycles. The exception to this is retroreflector E1. Retroreflector E1 was the first retroreflector that was tested and was the test case for when the design of the thermal chamber was being finalized. Because of this, it had been thermally cycled dozens of times before a complete thermal cycle to 185 K could be done. After this retroreflector had been thermally cycled three times, the initial and final dihedral angles would be within measurement error. This is typically what was seen with the epoxy cubes. The first 1–2 thermal cycles of the epoxy-bonded retroreflectors would change dihedral angles in an uneven manner but would return close to what they originally started from. This can be seen by comparing the values of the fourth column of Table 2. The amount of change in the original dihedral angles to the final dihedral angles typically decreases after the first 1–2 thermal cycles, until it was within measurement error. The initial change in dihedral angle error is attributed to stresses being released in the epoxy as it is being thermally cycled. As the epoxy is thermally cycled more and more, there is less and less stress within the bond, so it begins to "settle down."

Both the change in wavefront and change in MBD had trends that followed the change in the dihedral angle errors; the larger the dihedral angle change, the larger the change in wavefront and MBD. This trend holds for E1, E2, and E3, but not for E4. When comparing E2 and E4, it can be seen that the change in dihedral angle errors are the same, but E4 has a change in wavefront about half of that of E2 and almost twice the change in MBD as E2. The authors speculate that this is most likely due to the design of E4. As stated above, E4 had a design that incorporated a groove down the center of the bonding seam that the epoxy was applied to. This design was used to try and counteract the flowering effect of the other epoxy-bonded retroreflectors. By adding the second bonding seam, the forces incurred when thermally cycling the retroreflector would hopefully cancel out. When E4 was being thermally cycled, stresses in the mirrors could be inferred through the curvature of the lines in the interferogram. These stresses could be causing the mirrors to warp, which would lead to a

Table 2. Data for the Thermally Cycled Epoxy-Bonded Retroreflectors

		Total Dihedral Angle Change (arc sec)		Wavefront Change (Waves at 633 nm)		MBD (arc sec)	
Retro	Tested Days Later	195 K	295 K	195 K	295 K	195 K	295 K
E1	253	19.0	0.3	3.76	0.10	26.0	0.2
E2	162	10.4	0.7	4.48	0.39	7.6	0.2
E2	165	10.0	0.1	4.59	0.08	7.3	0.3
E2	166	9.9	0.2	4.51	0.11	4.9	0.2
E3	176	26.2	0.6	6.23	0.15	34.7	0.8
E3	178	25.3	0.7	6.34	0.43	33.9	1.9
E3	181	24.1	0.3	5.76	0.24	32.7	0.6
E4	34	9.9	0.2	2.35	0.00	13.3	0.1
E4	35	9.7	0.1	2.27	0.03	13.1	0.1
E4	36	9.7	0.2	2.26	0.10	13.0	0.1
Average		15.4		4.26		18.6	
Std. Dev.		7.3		1.58		11.9	

Table 3. Data for Thermally Cycled HCB-Bonded Retroreflectors

Retro	Tested Days Later	Total Dihedral Angle Change (arc sec)		Wavefront Change (Waves at 633 nm)		MBD (arc sec)	
		195 K	295 K	195 K	295 K	195 K	295 K
HCB1	76	5.3	0.4	1.04	0.02	1.5	0.7
HCB1	77	5.0	0.4	0.94	0.06	0.2	0.9
HCB1	78	4.6	0.2	0.74	0.05	1.3	0.8
HCB2	86	5.7	8.8	1.27	0.95	7.6	10.8
HCB2	87	3.5	8.1	0.24	0.48	4.8	0.0
HCB2	93	3.5	3.7	0.10	0.17	4.2	0.5
HCB2	94	4.1	3.9	0.05	0.76	4.3	4.8
HCB3	63	5.5	4.5	1.47	1.10	9.1	8.7
HCB3	64	4.7	2.5	1.19	0.39	7.7	2.7
HCB3	65	4.6	0.7	1.09	0.16	7.5	0.2
Average		4.7		0.81		4.8	
Std. Dev.		0.8		0.51		3.1	

larger MBD. Due to the low number of retroreflectors made, more data points are needed before a definitive conclusion can be made.

B. HCB-bonded Retroreflectors

The results of thermally cycling the HCB retroreflectors are presented in Table 3. In one case (HCB1), the dihedral angles, after being thermally cycled, were within measurement error for all three thermal cycles. In another case (HCB2), the dihedral angles changed by a significant amount after being thermally cycled. The exact cause of this is unknown, but it is speculated that HCB2 most likely did not bond very well. Both retroreflectors had been monitored with an interferometer for approximately six weeks after they had been taken out of the bonding fixture. In the case of HCB1, the interferogram changed over time but slowly settled down. In the case of HCB2, even after six weeks, the interferogram was still changing a small, but noticeable, amount. This implies that either a good bond had not formed or there was a significant amount of stress built up within the bonds. If there was a significant amount of buildup of stress during the bonding process that was being released while being thermally cycled, then a behavior similar to that of the epoxy-bonded retroreflectors should be seen. This was not observed, so it is assumed that the unpredictable changes in the dihedral angles while being thermally cycled were the result of poor bonds. In the case of HCB3, there was a significant change in the dihedral angle errors after the first thermal cycle, but not in the following thermal cycles. The change is attributed to stresses being released within the bond since it acted in a similar manner to the retroreflectors that were bonded with epoxy.

Despite the fact that HCB2 had a significantly larger change in initial and final dihedral angles than the rest of the hydroxide-bonded retroreflectors, the HCB retroreflectors performed better than their epoxy counterparts. The average dihedral angle error change was about one third that of the epoxy-bonded retroreflectors, the change in wavefront was about one fifth of the epoxy-bonded retroreflectors, and the change in MBD was about one fourth that of the epoxy-bonded retroreflectors (although still within statistical error of each other). This is expected, as the CTE of HCB is assumed to be less than that of the epoxy used. What wasn't expected with the HCB cubes was the large amount of irreversible deformation that occurred when thermally cycling. This deformation was significantly more than when epoxy was used, and the authors attribute it to the rough bonding surface that was used since this effect wasn't seen when a flat and smooth surface was used (as will be discussed later).

Table 4. Data for the Thermally Cycled Hybrid-Bonded Retroreflectors

Retro	Tested Days Later	Total Dihedral Angle Change (arc sec)		Wavefront Change (Waves at 633 nm)		MBD (arc sec)	
		195 K	295 K	195 K	295 K	195 K	295 K
H1	50	11.7	0.7	1.10	0.43	12.8	2.3
H1	51	11.4	1.7	0.79	0.40	12.3	2.2
H1	52	11.7	2.6	0.81	0.08	12.6	0.2
H2	14	5.9	11.5	0.13	2.01	2.4	13.7
H2	15	9.2	0.7	1.69	0.47	5.0	0.4
H2	17	9.0	0.6	1.30	0.06	5.1	0.4
H3	29	4.1	1.4	0.44	0.09	0.0	1.9
H3	30	4.2	2.0	0.65	0.01	0.2	1.3
H3	31	4.9	6.2	0.44	1.08	1.5	6.2
Average		8.0		0.82		5.8	
Std. Dev.		3.3		0.48		5.4	

Table 5. Data for the Thermally Cycled Fused Silica Retroreflectors Bonded with HCB

Retro	Tested Days Later	Total Dihedral Angle Change (arc sec)		Wavefront Change (Waves at 633 nm)		MBD (arc sec)	
		195 K	295 K	195 K	295 K	195 K	295 K
FS1	58	0.4	0.1	0.16	0.06	0.4	0.1
FS1	59	0.6	0.1	0.16	0.04	0.3	0.1
FS1	63	0.6	0.4	0.25	0.12	0.3	0.1
FS2	61	2.6	0.6	0.76	0.58	3.8	0.5
FS2	62	3.6	1.4	0.52	0.13	4.5	0.3
FS2	63	3.1	0.3	0.65	0.10	4.3	0.0
Average		1.8		0.42		2.3	
Std. Dev.		1.5		0.26		2.1	

From the data in Tables 2 and 3, it appears that there is not a correlation between how much time passes between when the retroreflector was assembled and when it was thermally cycled and how much the retroreflector changed. This is most likely due to the fact that the epoxy used fully cures after approximately two weeks and that the HCB is typically set after four weeks. In all cases, the retroreflectors were tested after the amount of time for the bond to fully set. If the retroreflectors were tested before this time, then a different behavior would be expected.

C. Hybrid-Bonded Retroreflectors

The results of thermally cycling the hybrid-bonded retroreflectors are presented in Table 4. Despite only one retroreflector being made of each design for the hybrid-bonded retroreflectors, significant information can be gleaned from their behavior. In the case of H1, the epoxy was only applied to half the thickness of the mirror and then the sodium silicate solution was applied after that. A visual inspection of the bond area showed that less than 10% of the total bond area had been hydroxide bonded. When the retroreflector was thermally cycled, the wavefront and dihedral angles changed in the opposite direction from those that were only epoxy bonded. The reason the retroreflector "closed in" instead of flowering out is because the epoxy is now acting like a hinge in the opposite direction. The addition of the hydroxide solution was to form a bond that would impede the hinging action of the epoxy. Unfortunately, the small percentage of area that bonded when HCB was used was not enough to significantly impede the hinging action of the epoxy.

In the case of H2, the retroreflector had the hydroxide solution applied only 14 days before it was thermally cycled. From the data, we can see that it behaved in a similar manner to that of HCB3, with the first thermal cycle causing the retroreflector to change significantly more than the following two thermal cycles. Since the hydroxide bond had most likely not fully cured [17], this effect was most likely from stresses that had not completely dissipated before being tested.

When H3 was bonded, the hydroxide solution was applied down the groove in the middle of the mirror (see Fig. 2). This allowed the solution to spread out in an even manner and bond equally on both sides of the groove. When bonding the other HCB retroreflectors, the solution was applied with a brush from the back and wicked in. Although the solution would wick in throughout most of the bonding surface, a fillet would form on the backside and form a chemical bond. It is believed that this was one of the primary causes for the retroreflectors to change when bonding. The amount of change that would occur during bonding would typically be several tens of arc seconds to over a hundred arc seconds. When bonding H3, very little active alignment was actually needed and significantly less than any of the other retroreflectors that had been made. Although H3 performed similarly to the other hydroxide-bonded retroreflectors, it appears that the change after being thermally cycled is for the worse. The cause for this is unknown.

D. Fused Silica Retroreflectors

In addition to the five Pyrex retroreflectors, two retroreflectors were made out of fused silica using the HCB method. One was made using a fixture (FS1) and one was made using a master cube (FS2). The data from thermally cycling these retroreflectors is presented in Table 5. It can be seen from Table 1 that both FS1 and FS2 had significantly lower dihedral angle errors, wavefront error, and MDB. This is assumed to be due to the polished bonding surfaces of the fused silica mirrors. The Pyrex mirrors had a ground bonding surface that was being bonded to a mirrored surface, while the fused silica mirrors had surfaces that were polished to better than $\lambda/8$ and the mirrored surface was perpendicular to the bonding surface to better than 3 arc sec. Even without any active alignment while in the fixture, the fused silica retroreflectors still bonded significantly better than those made of Pyrex.

Although the mean values of the dihedral angle errors, the change in wavefront, and the MBD are roughly half those of the HCB Pyrex retroreflectors, for the wavefront and MBD, the values were still within statistical error. In the case of FS1, when thermally cycled, all measured properties were within the measurement error of the interferometer (± 0.4 arc sec for the dihedral angle error, ± 0.50 waves for the wavefront, and ± 1 arc sec for the MBD). When compared to the CIRS cube [19], FS1 showed changes in the dihedral angle errors that were a factor of approximately 5 less, and a MBD almost a

factor of 2 less. The change in wavefront was comparable. In the case of FS2, the majority of the changes that occurred were for one dihedral angle only. The exact cause of this is unknown and more retroreflectors are needed before a definitive conclusion can be made. Although FS2 showed a change in dihedral angle errors similar to those of the CIRS cube [19], the wavefront change was approximately a factor of 2 worse, and the MBD was approximately a factor of 6 worse.

E. Discussion

When comparing the epoxy-bonded and HCB Pyrex retroreflectors, we found that the average change in dihedral angles, wavefront, and MBD were all less when using HCB. It is assumed that this is due to HCB having a lower differential CTE between the bonding material and the mirror substrate. This hypothesis is strengthened by the fact that the average change for the fused silica retroreflectors is less than that of the Pyrex retroreflectors. If the CTE of HCB was limiting the change of the retroreflector, then the fused silica retroreflectors should have changed by a similar amount to that of the Pyrex retroreflectors. From our results we see that this is not the case, although more statistics are needed before a definitive conclusion can be made.

It was also found that there were irreversible effects, when thermally cycling the HCB Pyrex retroreflectors, that were not seen with the fused silica retroreflectors, and this is attributed to the rough bonding surface of the Pyrex. More test samples and repeated thermal cycling are needed to determine the exact cause of the irreversible effects. Additional environmental tests, such as shock and vibration testing, will need to be done to ensure that HCB-bonded retroreflectors can survive the harsh conditions experienced during launch without significant changes to the retroreflector.

The performance of the hybrid-bonded retroreflectors is between that of the epoxy-bonded and HCB retroreflectors. Due to only testing one retroreflector of each design, it is hard to draw any specific conclusions, but what can be said for the hybrid method is that the alignment after adding the hydroxide solution was significantly easier than when the epoxy joints were not used. It may be possible to use a modified version of this to increase the precision to which the dihedral angles could be set when using the HCB method.

Although other retroreflector designs, such as a tongue-and-groove design [19] and epoxies with lower CTEs, may produce better results, there will still be some residual stresses from the epoxy curing that will be let out as the retroreflector is thermally cycled. The extent to which this happens cannot always be kept constant and will cause one retroreflector to behave differently from the next. The extent to which this happens with HCB retroreflectors is still unknown due to the low number of retroreflectors that have been bonded using this method, but initial results look promising. Two of the three retroreflectors changed very little when thermally cycled, and it is speculated that the third retroreflector most likely did not bond very well, which caused the outlying results. Overcoming the inability to bond the dihedral angles to the precision to which they are needed for LLR will be a major hurdle to overcome.

5. Conclusion

We have shown that retroreflectors bonded using the HCB process produced changes in the dihedral angle errors, wavefront, and MBD less than those when the Epon/Versamid epoxy was used and thermally cycled over the same temperature range. In addition, we were able to produce a single retroreflector that, when thermally cycled, changed less than that of the CIRS cube on the Cassini mission. The hybrid method made it easier to align the mirrors when hydroxide bonding was used, but did not produce as good results when thermally cycled as when only the HCB method was used. Although the changes were less when HCB was used, the precision to which the dihedral angles can be bonded still needs to be significantly improved if hollow retroreflectors are to be used for LLR, as subarc second dihedral angle accuracy will likely be required for lunar cubes to maintain their high lidar cross-section. Smooth and perpendicular bonding surfaces will undoubtedly be necessary, as well as other improvements to the bonding technique. If this challenge can be overcome, then HCB hollow retroreflectors, particularly those made out of an ultralow CTE material such as ULE or Zerodur, show real promise for the next generation of LLR.

This research was supported by an appointment to the NASA Postdoctoral Program at the Goddard Space Flight Center, administered by Oak Ridge Associated Universities through a contract with NASA. The authors would like to thank Thomas Zagwodski and Michael Perry for their contributions in setting up the fabrication and testing facility at the Goddard Geophysical and Astronomical Observatory. S. M. M. is a member of the LUNAR consortium (http://lunar.colorado.edu), headquartered at the University of Colorado, and funded by the NASA Lunar Science Institute (via Cooperative Agreement NNA09DB30A) to investigate concepts for astrophysical observatories on the Moon.

References

1. S. Merkowitz, "Tests of gravity using lunar laser ranging," Living Rev. Relativity **13**, 7 (2010).
2. T. W. Murphy, "Lunar laser ranging: the millimeter challenge," Rep. Prog. Phys. **76**, 076901 (2013).
3. T. W. Murphy, Jr., E. Adelberger, J. Battat, C. Hoyle, R. McMillan, E. Michelsen, R. Samad, C. Stubbs, and H. Swanson, "Long-term degradation of optical devices on the Moon," Icarus **208**, 31–35 (2010).
4. S. M. Merkowitz, P. W. Dabney, J. C. Livas, J. F. McGarry, G. A. Neumann, and T. W. Zagwodzki, "Laser ranging for gravitational, lunar, and planetary science," Int. J. Mod. Phys. D **16**, 2151–2164 (2007).
5. T. W. Murphy, Jr., E. Adelberger, J. Battat, C. Hoyle, N. Johnson, R. McMillan, E. Michelsen, C. Stubbs, and H. Swanson, "Laser ranging to the lost Lunokhod 1 reflector," Icarus **211**, 1103–1108 (2011).

6. P. Bender, D. Currie, R. Dicke, D. Eckhardt, J. Faller, W. Kaula, J. Mullholland, H. Plotkin, S. Poultney, E. Silverberg, D. Wilkinson, J. Williams, and C. Alley, "The lunar laser ranging experiment," Science **182**, 229–238 (1973).
7. J. G. Williams, S. G. Turyshev, and D. H. Boggs, "Lunar laser ranging tests of the equivalence principle," Class. Quantum Grav. **29**, 184004 (2012).
8. T. W. Murphy, Jr., E. Adelberger, J. Battat, C. Hoyle, R. M. N. Johnson, C. Stubbs, and H. Swanson, "APOLLO: millimeter lunar laser ranging," Class. Quantum Grav. **29**, 184005 (2012).
9. D. Currie, S. DellAgnello, and G. D. Monache, "A lunar laser ranging retroreflector array for the 21st century," Acta Astronaut. **68**, 667–680 (2011).
10. S. Goodrow and T. Murphy, "Effects of thermal gradients on total internal reflection corner cubes," Appl. Opt. **51**, 8793–8799 (2012).
11. D. Gwo, S. Wang, K. Bower, D. Davidson, P. Ehrersberger, L. Huff, E. Romero, M. Sullivan, K. Triebes, and J. Lipa, "The gravity Probe-B star-tracking telescope," Adv. Space Res. **32**, 1401–1405 (2003).
12. D. Gwo, "Ultra-precision bonding for cryogenic fused-silica optics," Proc. SPIE **3435**, 136–142 (1998).
13. D. Gwo, "Hydroxide-catalyzed bonding," U.S. patent 6548176 (April 15, 2013).
14. P. Mammini, "A bonded precision optical assembly using potassium hydroxide," Proc. SPIE **7425**, 74250O (2009).
15. A. Preston, B. Balaban, and G. Mueller, "Hydroxide-bonding strength measurements for space-based optical missions," Int. J. Appl. Ceram. Tech. **5**, 365–372 (2008).
16. A. Preston and G. Mueller, "Bonding SiC to SiC using a sodium silicate solution," Int. J. Appl. Ceram. Tech. **9**, 764–771 (2012).
17. E. Elliffe, J. Bogenstahl, A. Deshpande, J. Hough, C. Killow, S. Reid, D. Robertson, S. Rowan, and G. Cagnoli, "Hydroxide-catalysis bonding for stable optical systems for space," Class. Quantum Grav. **22**, S257–S267 (2005).
18. N. Beveridge, A. Van Veggel, M. Hendry, P. Murray, R. Montgomery, E. Jesse, J. Scott, R. Bezensek, L. Cunningham, J. Hough, R. Nawrodt, S. Reid, and S. Rowan, "Low-temperature strength tests and SEM imaging of hydroxide catalysis bonds in silicon," Class. Quantum Grav. **28**, 085014 (2011).
19. J. Lyons and P. Hayes, "High-optical-quality cryogenic hollow retroreflectors," Proc. SPIE **2540**, 94–100 (1995).